Some Navier-Stokes Calculations for the CAST-10 Airfoil

D. Schwamborn
DLR, Institute for Theoretical Fluid Mechanics
Bunsenstr.10, 3400 Göttingen, FRG.

Introduction

Numerical methods for viscous transonic aerodynamics have made enormous progress in recent years, but further improvement is still needed, especially with regard to the accuracy of the prediction. This improvement will mainly result from validation of codes based on data from appropriate transonic experiments, where e.g. boundary conditions to be used in the calculation have to be measured and where also shear stress data or velocity profiles are available. Because there are not enough such experiments it is also necessary to compare numerical results with data from experiments which don't meet the requirements of code validation. Even in these cases a lot of useful information can be gained, not only for the theoretician but also for the experimentalist.

In the following a comparison is presented between the computed results of the flow about the CAST10 airfoil and the pressure distributions and force coefficents from experiments in the adaptive TCT [1].

Description of the Method

For the discretization of the complete Navier-Stokes equations a finite volume Runge-Kutta time-stepping scheme based on a cell centered formulation is used [2]. Since the fluxes across the cell faces are averaged from neighbouring cells which is equivalent to central differencing artificial diffusion terms are needed. These damping terms are the usual blend of second and fourth order differences except that a weighting function is employed. This weighting function restricts the artificial diffusion in the viscous near-wall regions or in the wake, where the unweighted formulation would otherwise result in a predominance of non-physical diffusion.

The set of ordinary differential equations resulting from the finite volume discretization is integrated in time using a linearized four-stage Runge Kutta scheme. Local time stepping is employed to accelerate the convergence to steady-state solutions, and in order to save further computation time the artificial and physical diffusion terms are updated only once per time step reducing the execution time by more than 50 per cent.

To have a well-posed problem a set of appropriate boundary conditions is needed. At the airfoil surface the no-slip and the adiabatic wall condition is used. The pressure is derived from the assumption of zero pressure gradient normal to the wall which is justified for the very small step sizes normal to the wall used in Navier-Stokes calculations for turbulent flows. At the far field boundary we use one-dimensional Riemann invariants normal to the boundary in order to obtain boundary conditions.

Since the two-dimensional flow solver used here is derived from the three-dimensional one described in [2], it allows for a block-structured approach, i.e. the computational domain can be divided in a number of subdomains called blocks. The advantage of this approach is that it is very flexible regarding the handling of complex geometries (e.g. with multiply connected domains). The flexibility is partly due to the segmentation of the block faces, which allows for the use of different types of boundary conditions and different neighbouring blocks at each

block face. This feature was used in the present calculations to model the finite thickness of the CAST10 trailing edge by using a C-type mesh past the airfoil with an extra grid in the gap behind the trailing edge. For more information on the block structure refer to [2].
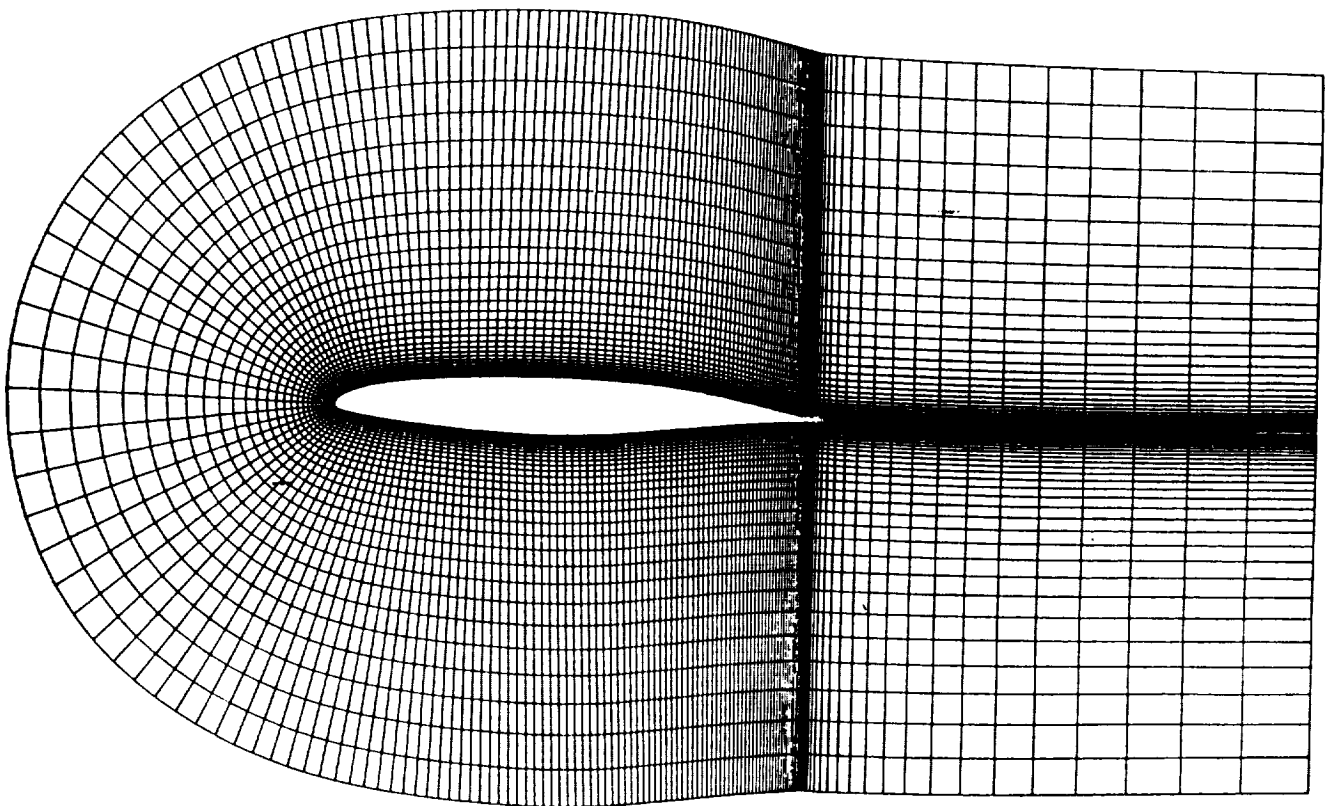
To simulate the turbulence the well-known algebraic model of Baldwin and Lomax [3] is used.

Typical grid in the vicinity of the airfoil

For the flow about the airfoil the mesh consists of 260x80 cells in chordwise and wall-normal direction, respectively and the mesh extends about 10 root chords away from the airfoil. There are 200 cells on the wing surface and the first step size normal to the wing surface is chosen such that it is equivalent to $z^+ \approx 2$ in the first cell of the wall, in order to resolve the laminar sublayer of the turbulent flow.
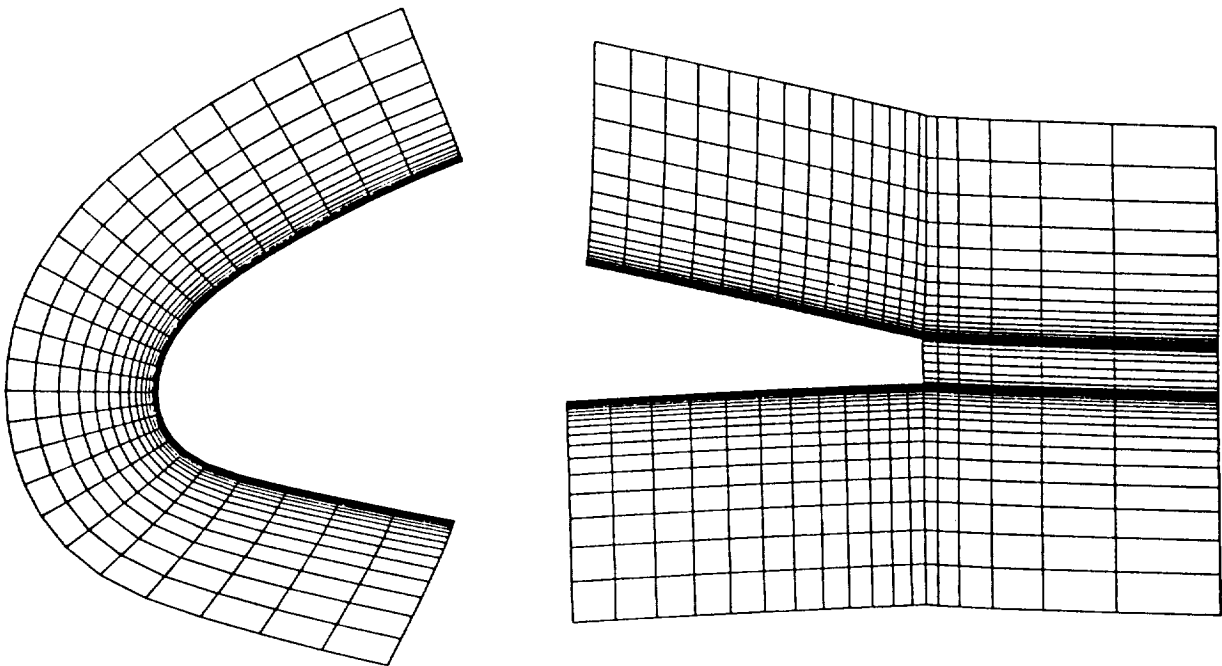
The C-type grid is generated algebraically using a code of Sobieczky [4] resulting in a mesh with a gap of the thickness of the trailing edge. This gap is closed by a suitable interpolation which yields a smooth distribution of the stepsize in the direction normal to the wake.

The block structure in the present calculations includes three blocks; the first and second corresponding to the C-type mesh in the vicinity of the airfoil and to the interpolated mesh in the gap, respectively. In these two blocks the complete Navier-Stokes equations are solved, whereas only the Euler equations are solved in the third block for the outer part of the C-mesh. The block boundary of the later block is about 25 per cent of chord away from the airfoil and the wake, respectively.

Details of the mesh near the leading and trailing edges

The figures show the strong clustering of the grid lines near the wall and give an idea of the grid in the gap behind the trailing edge. In the present calculation the mesh within the gap behind the trailing edge is fairly small, i.e. there are only ten cells over the height of the trailing edge.

Comparison of experimental and computed lift and drag

M = .73   Re = 10 million

The table shows a comparison of the lift and drag coefficients from experiments in the TCT [1] with free transition (the transition takes place somewhere near the leading edge) and calculations where the transition point is prescribed. The transition location is given as upper/lower chord position.

As can be seen from the table the upper surface location of transition (.07 to .2 chord) has almost no influence on the coefficients, but the lift increases when the transition location is shifted downstream on the lower surface (to .15 and .2 chord).

The calculation for $\alpha = 3.0$ is slightly unsteady, i.e. the residuals stay on a certain level in the separation zone behind the shock.
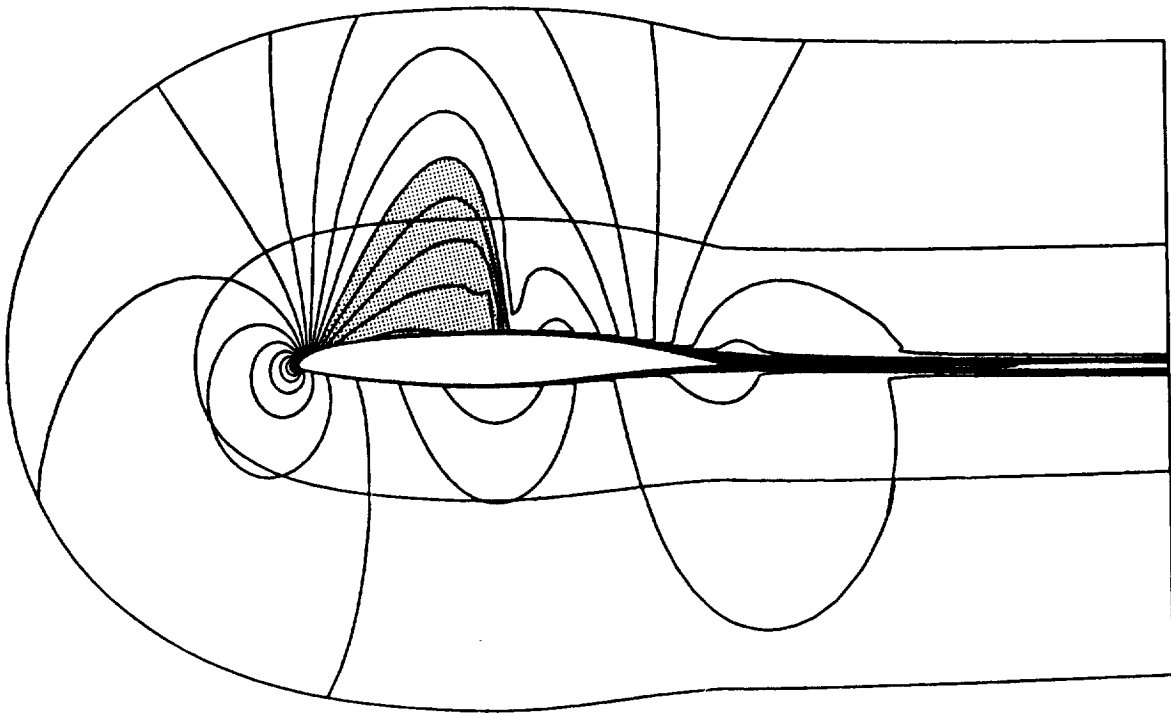
For details see the following pages.

α	exp./cal.	transition	lift coeff.	drag coeff.
1.0	exp.	free	.616	.010
	cal.	.07/.07	.677	.0152
	cal.	.10/.10	.677	.0152
	cal.	.15/.15	.685	.0149
	cal.	.07/.20	.695	.0150
	cal.	.20/.07	.677	.0150
	cal.	.10/.10 (modif.turb.)	.637	.0159
.9	cal.	.10/.10	.677	.0150
3.0	exp.	free	.895	.0450
	cal.	.10/.10	.82-.90	.033-.039

Iso-Mach contours for M= .73   Re= 10 million   α = 1.00

Calculation: transition at .10/.10 chord

This figure shows contour lines of the Mach number in the vicinity of the airfoil
(Δ= .05) with the supersonic regime set off in gray. Also shown are the block
boundaries of the computation. Since some isolines cross the boundary between
the viscous inner and the inviscid outer block without any disturbance it is obvi-
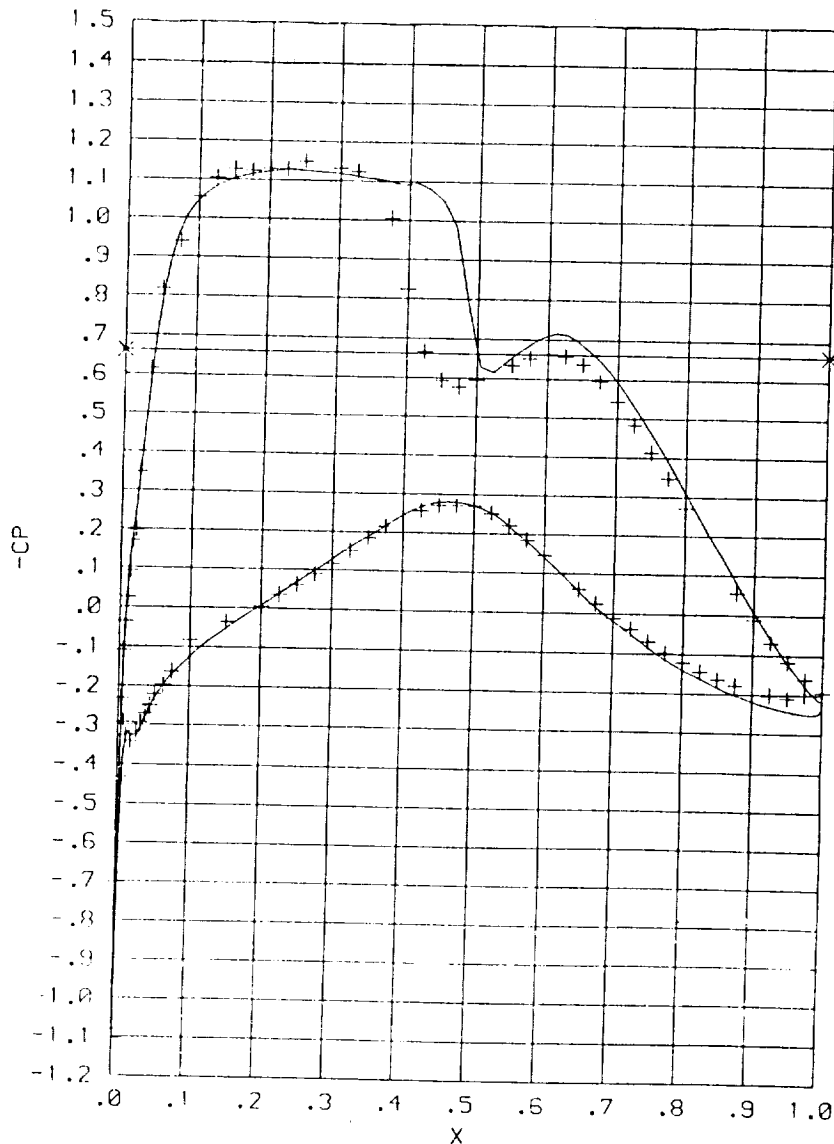ous that the block concept has no influence on the solution quality.

Cp-distribution at M = .73   Re = 10 million   α = 1.00

1. Calculation: transition at .10/.10 (or .07/.07) chord

The symbols show the experimental data from TCT [1](point 203) and the solid line shows the computational result. The horizontal line with the crosses at its ends indicates the critical Cp value. Fixing the transition at 10 or 7 per cent chord in the calculation gives the same pressure distribution.

The results compare quite well for the major part of the surface except near the trailing edge, but there is a discrepancy in the shock location of about 10 per cent chord.

To see the influence of the chosen transition location on the results the following variations are made.
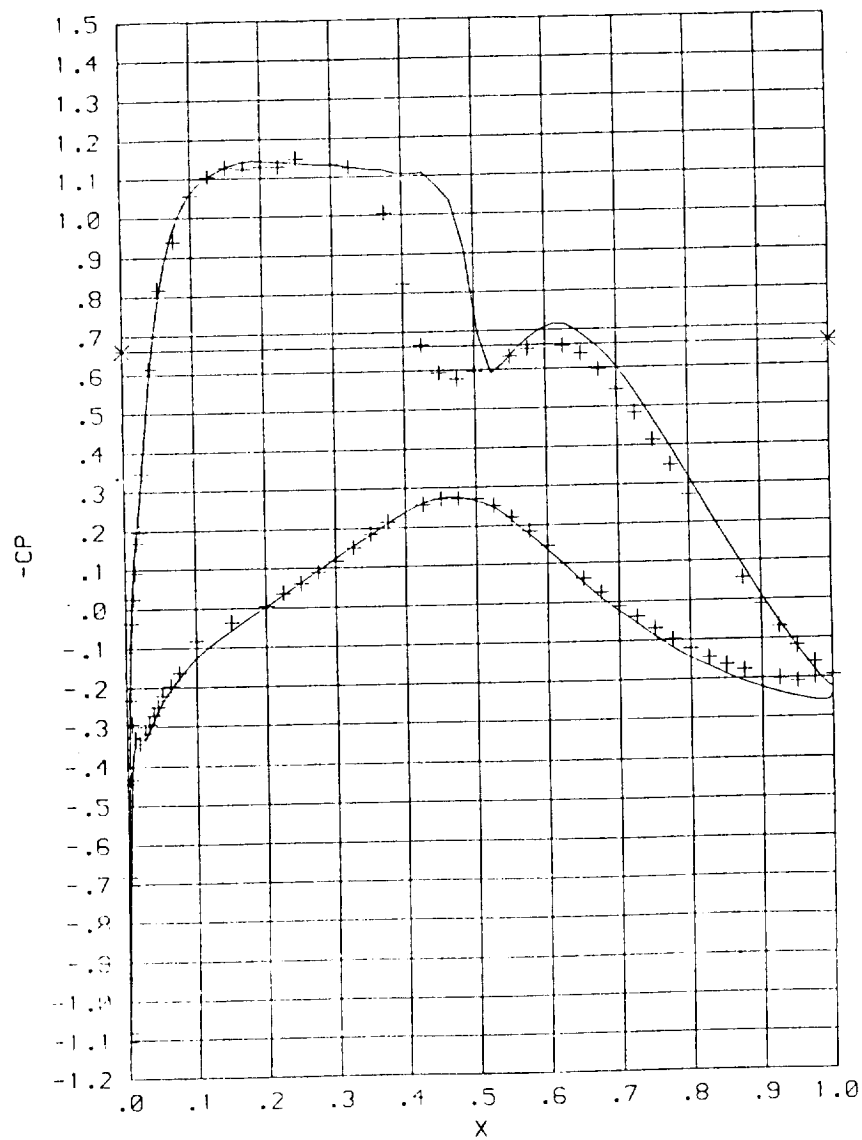
Cp-distribution M= .73   Re= 10 million   α = 1.00

2. Calculation: transition at .07/.20 chord

The pressure distribution shows almost no variation compared to previous calculation.
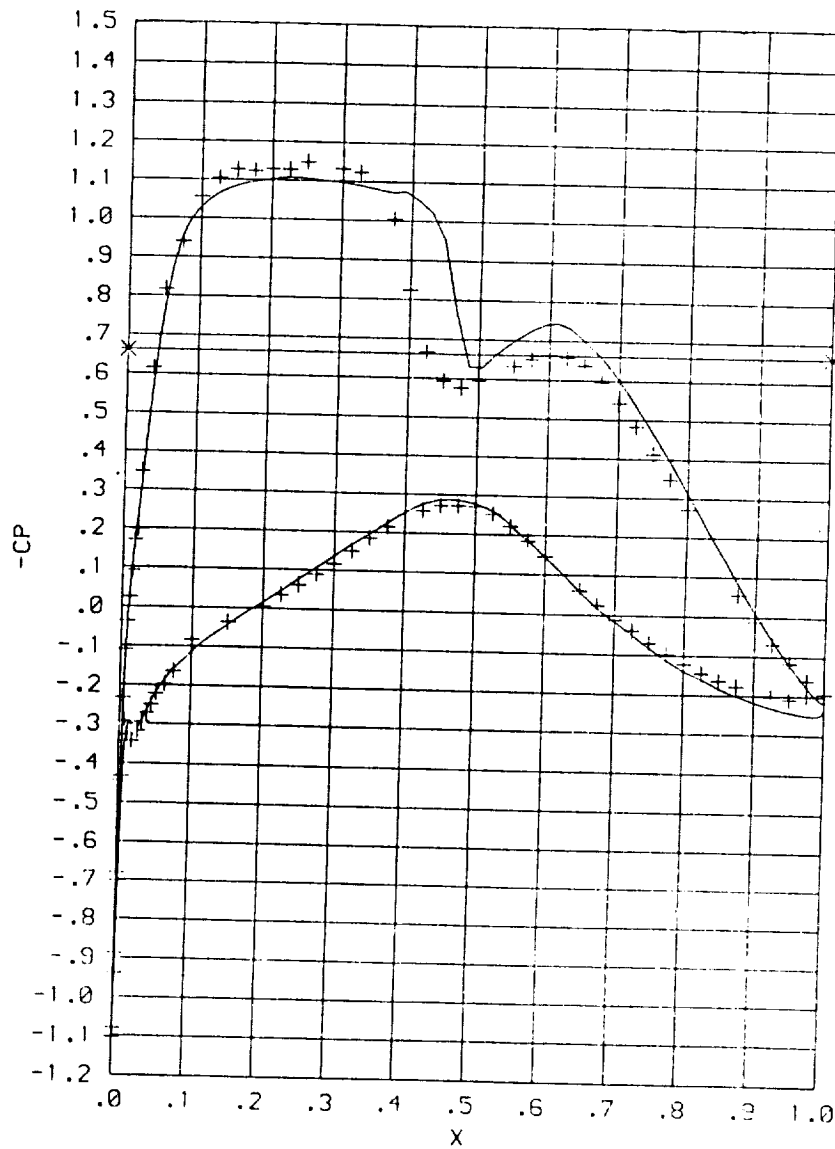
3. Calculation: transition at .20/.07 chord

The pressure at the beginning of the pressure plateau is now even closer to the experimental one, but the shock has moved a little bit further downstream. The solution behind the shock and at the lower surface are the same as before.

Cp-distribution M = .73   Re = 10 million   α = 1.00

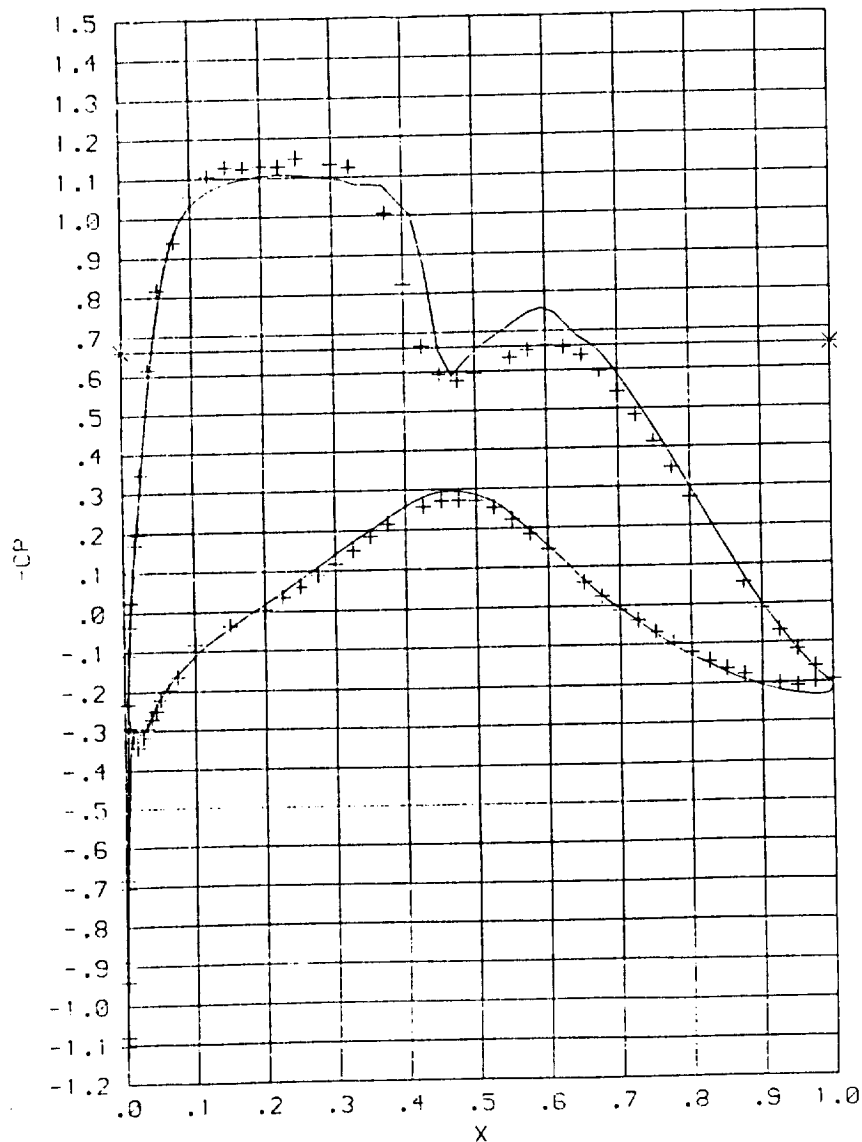*4. Calculation: transition at .10/.10 chord and α = .9*

A decrease in the angle of attack results in less agreement regarding the plateau pressure and the pressure at the lower surface. The shock has now moved upstream, but by a far too small extent. To match the plateau pressure again a higher Mach number would be necessary, but this further variation was not tried.

5. Calculation: transition at .10/.10 chord and variation of turbulence model near shocks
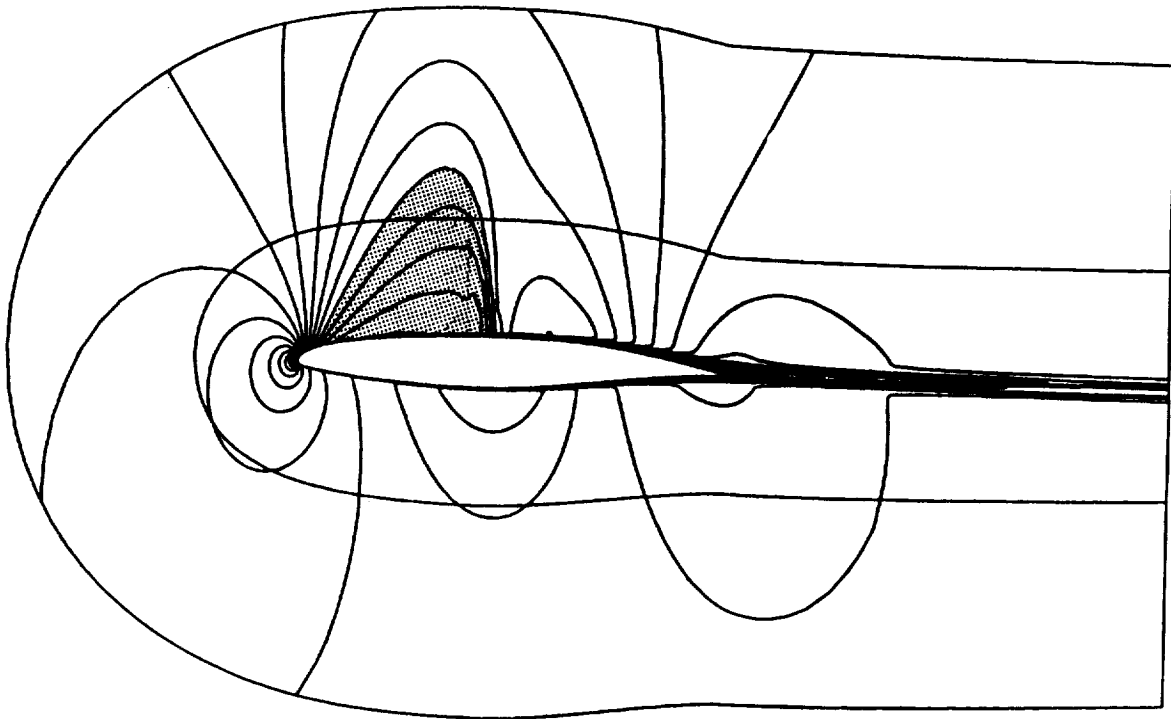
A modification in the Baldwin/Lomax turbulence model resulting in a local increase of the eddy viscosity is made. The shock is moved upstream almost into the right position but the plateau pressure and the pressure at the lower surface show now larger discrepancies similar to the result with the smaller angle of attack. It is obvious from the movement of the shock that there is a strong influence of the modelling on the turbulent shock boundary layer interaction.

Iso-Mach contours for M = .73 Re = 10 million α = 1.00

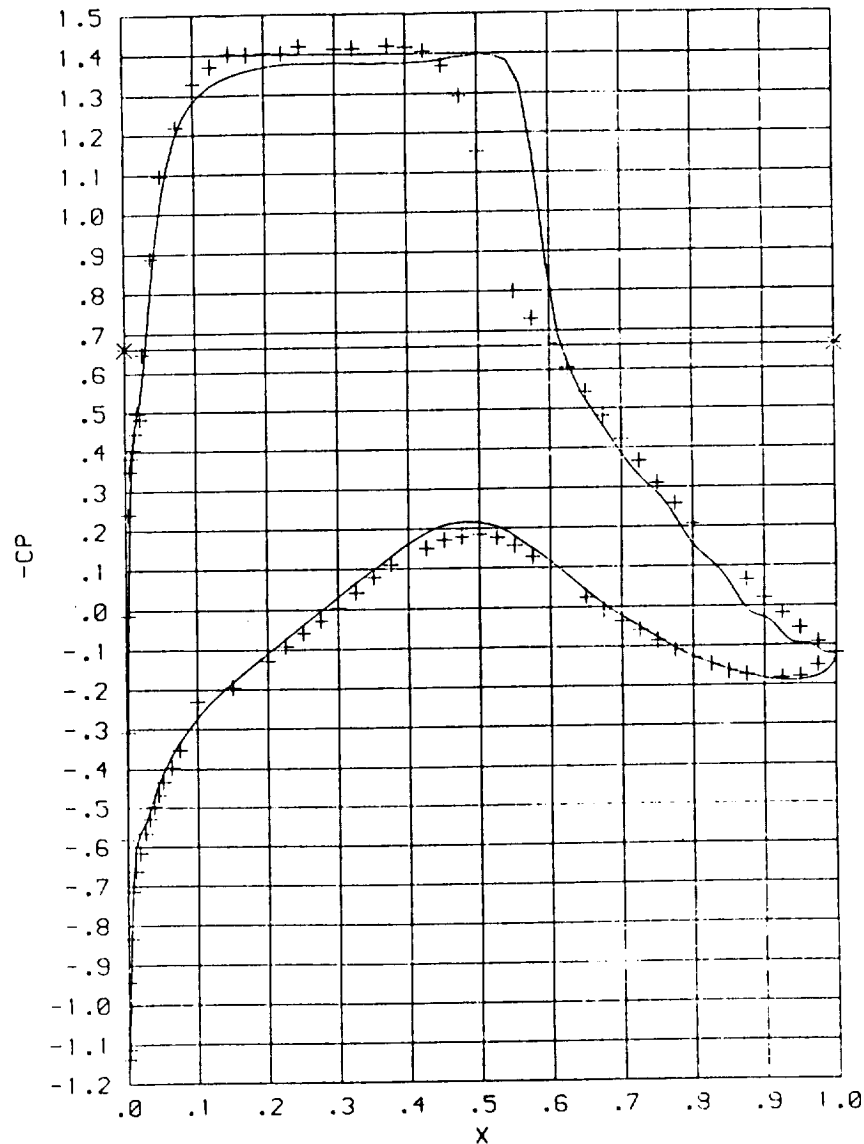*Calculation: transition at .10/.10 chord*
Modified turbulence model

This figure shows the Mach number distribution with the modified turbulence model. In comparison to the previous results one realizes the upstream movement of the shock due to this modification. Away from the supersonic region the two solutions look very similar as one could expect already from the pressure distributions.

Cp-distribution M = .73   Re = 10 million   α = 3.00
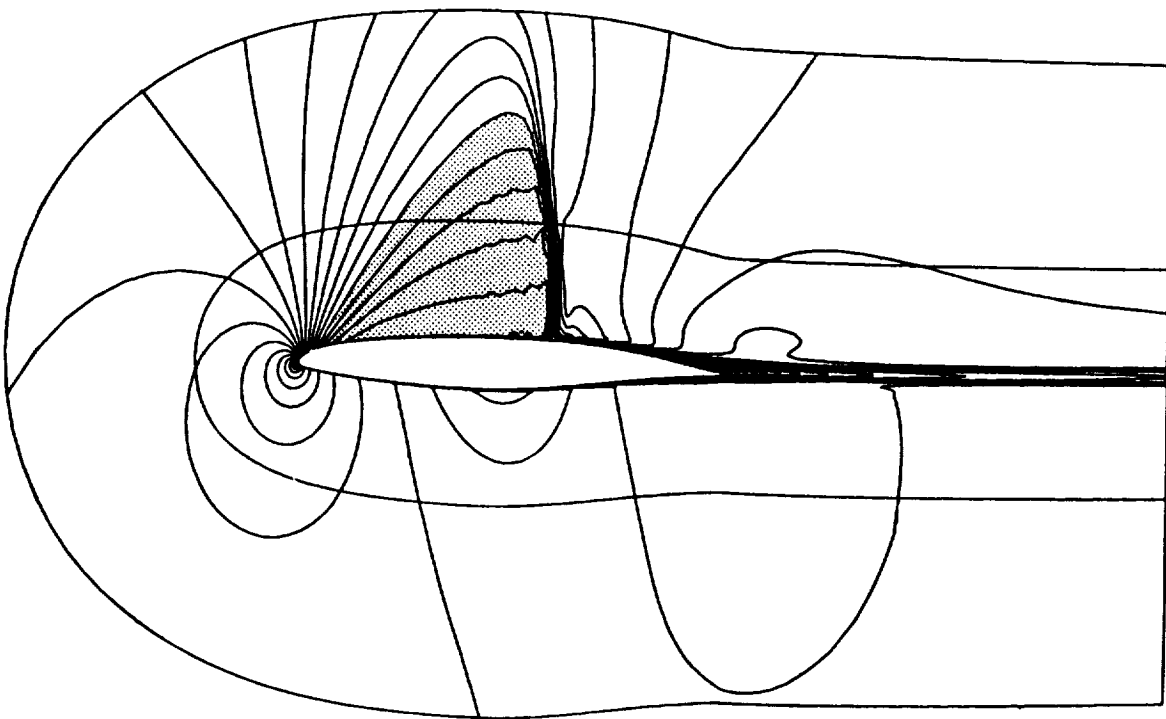
Calculation: transition at .10/.10 chord

For this higher angle of attack case (point 207 of TCT data[1]) the calculation indicates a slightly unsteady solution in the separated region on the upper surface near the trailing edge. Again the results compare quite well for the major part of the surface, but we find again the discrepancy in the shock location. In this case with separated flow the aforementioned modification of the turbulence model shows almost no influence on the solution, maybe because the modification is only local at the shock and does not extend over the whole separated region.

73

Iso-Mach contours for M= .73   Re= 10 million   α = 3.00

Calculation: transition at .10/.10 chord

This figure shows the Mach number distribution for the higher angle of attack case, where the shock has moved downstream. Due to the separation behind the shock the boundary layer has thickened considerably as can be seen in comparison to the Mach number distribution for α = 1.

Comparison of experimental and computed lift and drag at M= .765

The table shows a comparison of the force coefficients from experiments with fixed and free (for the higher Re numbers) transition to those from calculations where the transition location is always at .07/.07. Results are presented for different angles of attack and different Re numbers.

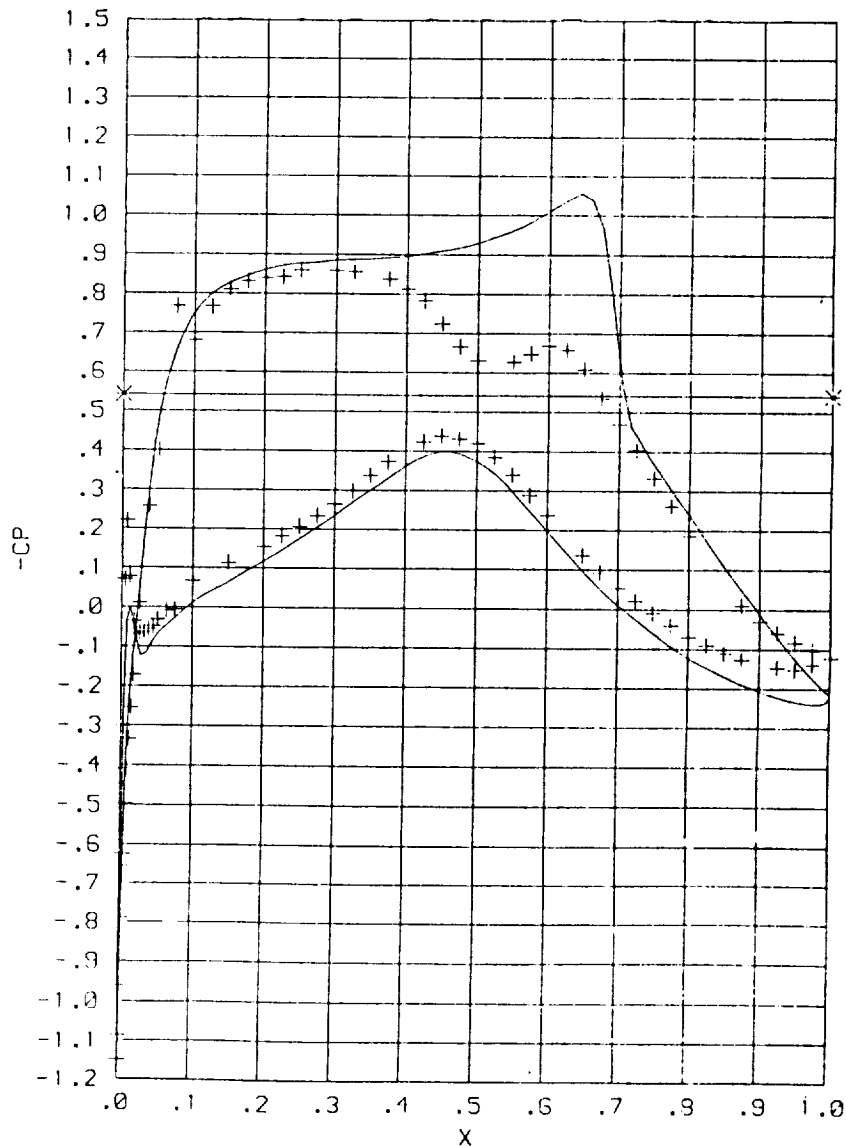For more details regarding the calculated results see the following pages.

α	Experiment lift / drag	Calculation lift / drag
Re = 4 million		
0	.378 / .012	.53 / .0169
.5	-	.604 / .0216
1.	.57 / .020	.53-.65 / .019-.028
Re = 10 million		
0	.45 / .011	.53 / .0155
.5	.588 / .015	.575 / .0185
1.	.623 / .024	.58-.63 / .019-0.25
Re = 40 million		
0	.538 / .012	.41-.43 / .010-.011

Cp-distribution M= .765 Re= 4 million α = 0.00

Transition at .07/.07 chord (calculation) and .06/.06 chord (experiment)

For this higher Mach number case (point 39 of TCT data [1]) the numerical result compares not so well with the experimental data, not even at the lower surface. The computation exhibits a pressure plateau with an expansion peak in front of the shock, whereas the experiment shows a double structure of weaker shocks. The calculated pressure distribution results in a higher lift (and drag) and in a higher trailing edge pressure.

According to previous experience the difference in the transition location between calculation and experiment is estimated to have practically no influence.
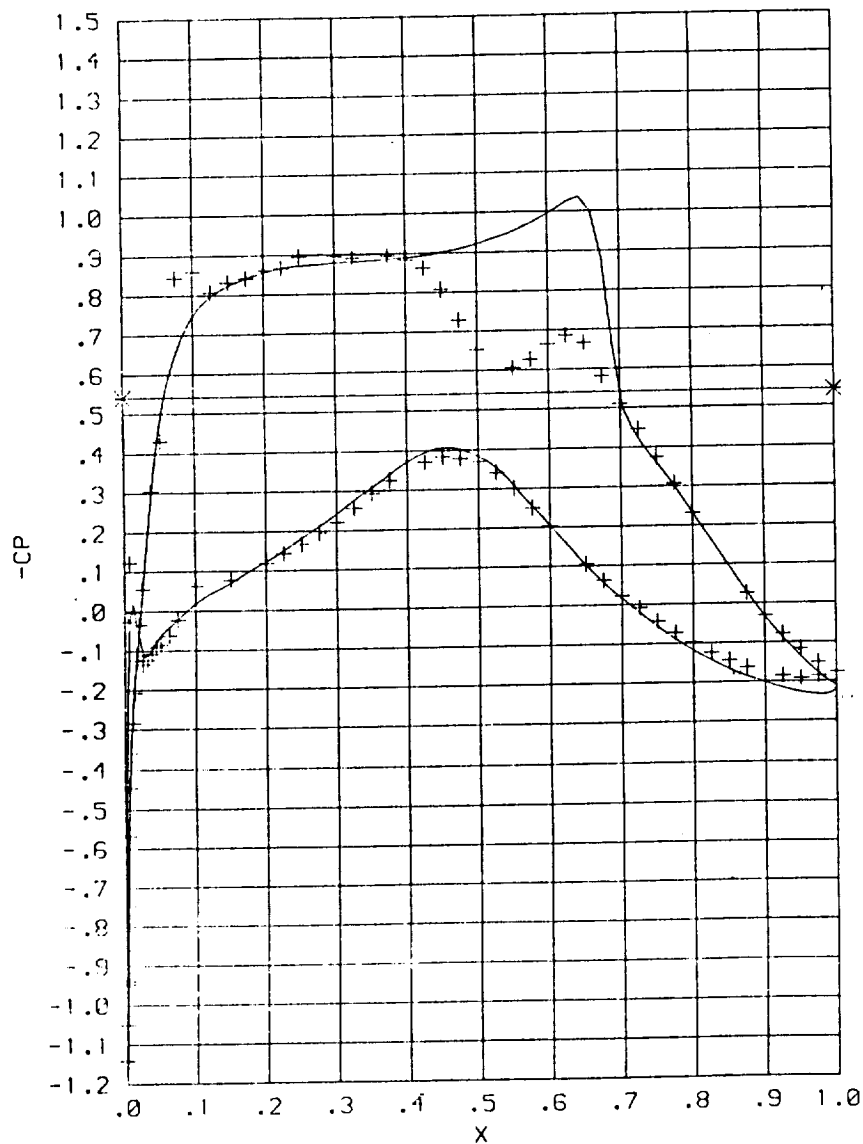
Cp-distribution M= .765 Re= 10 million α = 0.00

Transition at .07/.07 chord (calculation) and .06/.06 chord (experiment)

Increasing the Reynolds number results in almost no change in the computed pressure distribution. The experimental pressure (point 79 in TCT data [1]) is now slightly higher on the lower surface and slightly lower on the upper surface thus producing a higher lift due to the reduced decambering by the thinner boundary layers. Now the pressure distributions compare better except for the region of the shocks where we find again the double shock in the experimental data.
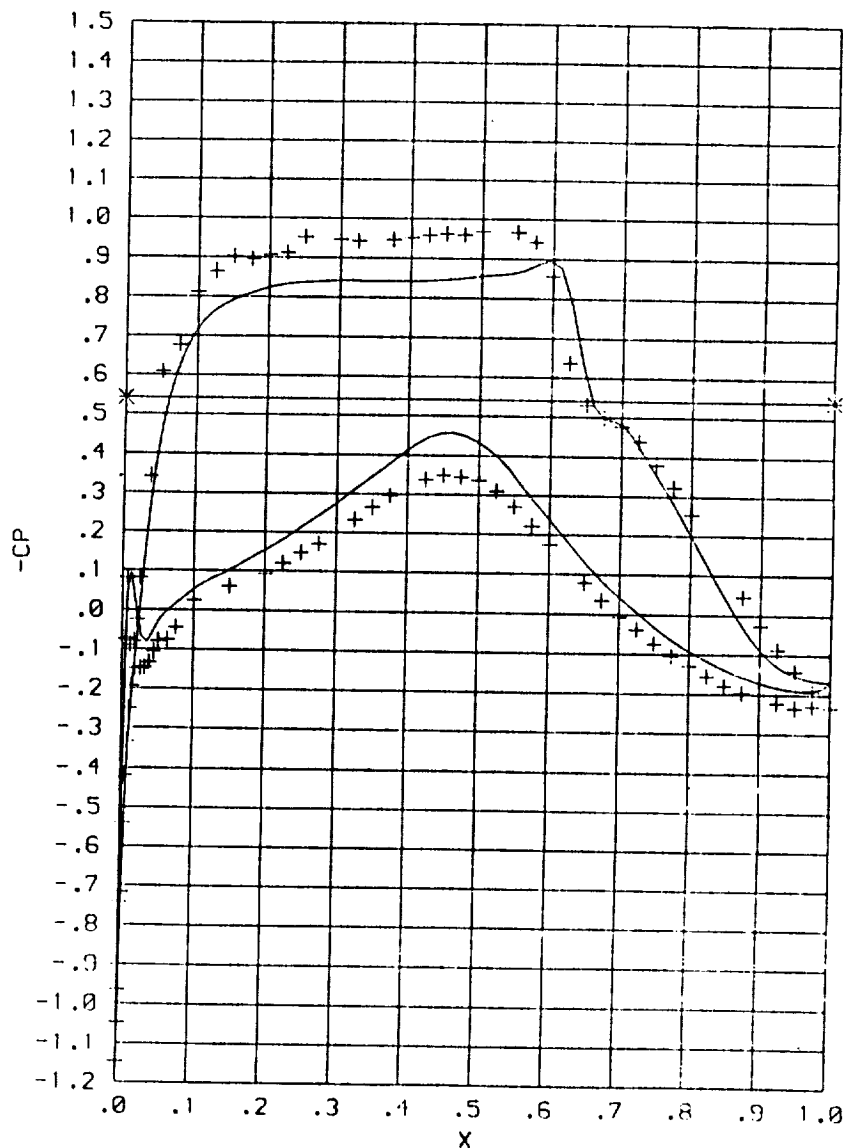
It is far from clear why the calculation at the lower Reynolds number doesn't show the decambering effect found in the experiment.

77

Cp-distribution M= .765 Re= 40 million α = 0.00

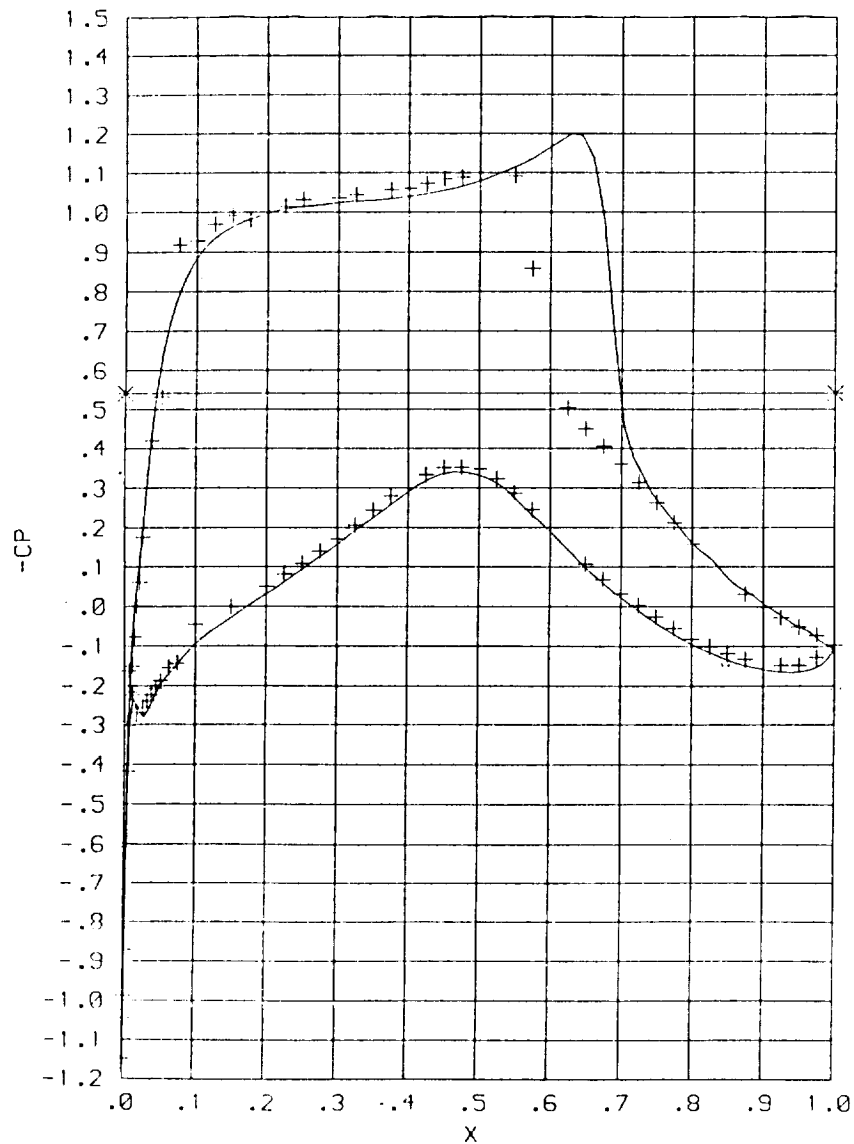*Transition at .07/.07 chord (calculation) and .06/.06 chord (experiment)*

A further increase in Reynolds number changes the situation in the experiment (point 284), i.e. the double shocks merge and form a stronger single shock downstream. Again the pressure is increased at the lower and decreased at the upper surface. Although the qualitative result of the computation compares now better to the experimental pressure distribution, the quantitative result is much worse. This is due to the poor resolution of the very thin boundary layer. With a better resolution, however, the computed shock position is again found downstream of the experimental one whereas the plateau pressure and the pressure at the lower surface are recovered. As for the lower Mach number cases we assume that this effect is at least partly due to the turbulent shock boundary layer interaction which is not correctly modelled by the Baldwin-Lomax turbulence model.

Cp-distribution M= .765 Re= 4 million   α = 1.00

Transition at .07/.07 chord (calculation) and .06/.06 chord (experiment)

For a higher angle of attack and the low Reynolds number (point 40 of TCT data [1]) we find only a single shock in the experimental data and, as is seen in most of the other cases, the numerical result compares quite well except at the shock. But this depends on the picked iteration cycle where the results are plotted, as will be discussed on the next page.
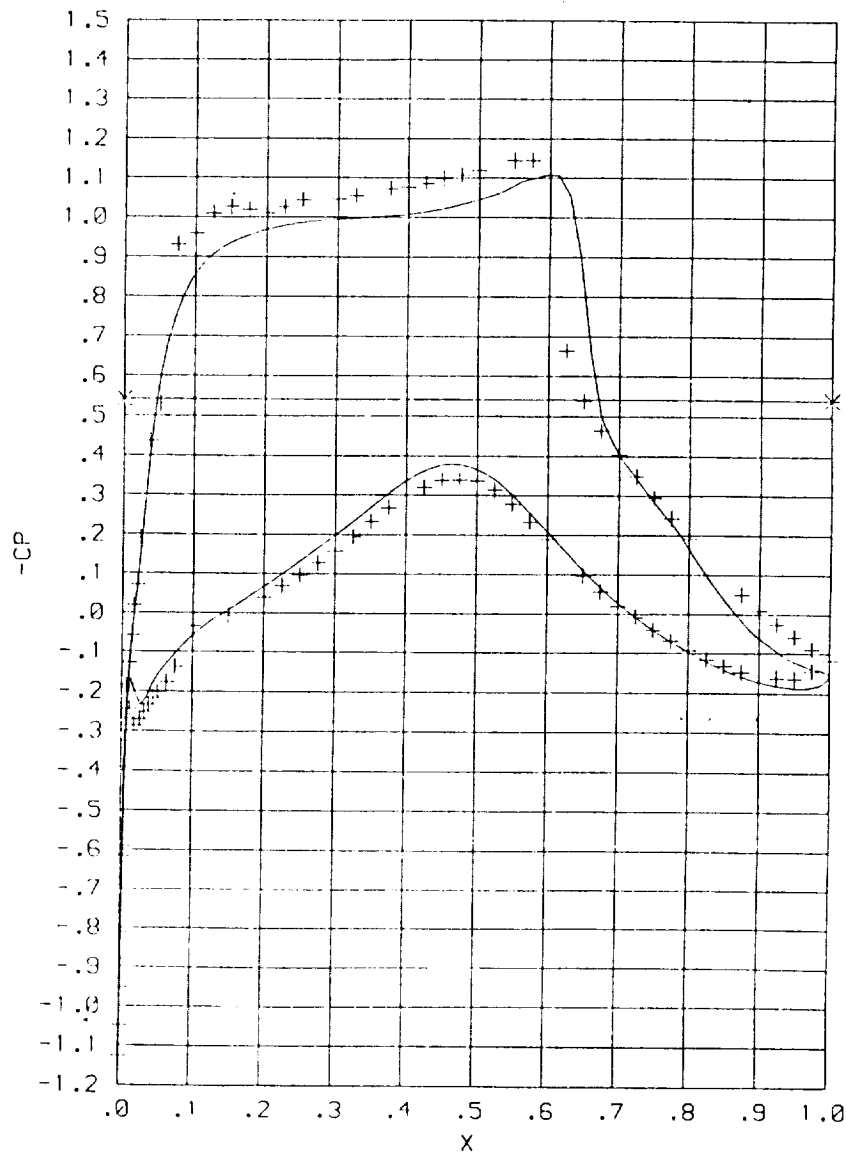
Cp-distribution M = .765 Re = 10 million α = 1.00

Transition at .07/.07 chord (calculation) and .06/.06 chord (experiment)

Increasing the Reynolds number again (point 339 of TCT data [1]) has little influence in the experimental data; only the shock is shifted downstream a little bit. One would expect the same for the computed results keeping in mind the results for zero incidence. But as is seen from the variation of lift and drag in the preceding table there is an unsteadiness in the numerical results at this angle of attack, i.e. the solutions do not converge to a steady state. The result shown here was obviously taken at a moment where the lift in the calculation was low, whereas the result on the previous page corresponds to a situation where the lift was high.

Since the numerical method uses local time stepping as an acceleration technique the unsteadiness cannot be interpreted in a physically meaningful way, although it indicates that a time accurate calculation at this angle of attack would yield an unsteady flow behavior, too.

Concluding Remarks

Results of the simulation of the viscous flow past the CAST10 airfoil have been shown for different flow conditions. Since the experiments provide only surface pressures and force coefficents the comparison to the numerical results relies on these.

Good agreement of the results is found for the lower Mach number cases except for the shock position. As numerical experiments indicate, this seems to be due to the turbulent shock boundary layer interaction which is not correctly modelled by the algebraic turbulence model employed.

For the lower Mach number case the influence of the transition location has been investigated, too. Changing the transition location at the lower surface has much more influence on the pressure distribution than changing it on the upper side.

For the higher Mach number case the double shock structure found in the experiment for the lower Reynolds numbers was not reproduced by the numerical solutions. The reason for this is unknown though it may be due to the turbulence modelling. For the higher Reynolds number a better resolution of the boundary layer is needed in the computation in order to recover the experimental pressure plateau; but then the shock position is still found downstream of the experimental one.

REFERENCES

[1] TCT data provided by E. Stanewsky, DLR-Institute for Experimental Fluid Mechanics, Göttingen.
The TCT is Described in:
Ladson, C.L., Ray, E.J.: Evolution, Calibration, and Operational Characteristics of the Two-Dimensional Test Section of the Langley 0.3 Meter Transonic Cryogenic Tunnel, NASA Technical Paper 2749, Sept. 1987.

[2] SCHWAMBORN, D.: Simulation of the DFVLR-F5 Wing Experiment Using a Block-Structured Explicit Navier-Stokes Method. Notes on Numerical Fluid Mechanics Vol.22, Vieweg Publishers,1988.

[3] BALDWIN, B.S., LOMAX, H.: Thin Layer Approximation and Algebraic Model for Separated Turbulent Flows. AIAA Paper 78-257, (1978).

[4] SOBIECZKY, H.: Analytical Surfaces and Grids. AGARDOGRAPH on Current Practices in Numerical Grid Generation